ISBN: 978-3-95450-211-0 doi:10.18429/JACoW-SRF2019-TUFUB5

EFFECTS OF STATIC MAGNETIC FIELDS ON A LOW-FREQUENCY TEM CLASS SUPERCONDUCTING CAVITY*

M. K. Ng#, M. P. Kelly, Z. A. Conway, K. W. Shepard
Argonne National Laboratory, Argonne, IL, USA

Abstract

Systematic studies on the effect of magnetic fields on a 337 MHz superconducting (TEM-mode) half-wave cavity are presented. The practical application of the results is for a possible future 2 K operation in the ATLAS heavy-ion accelerator at Argonne. The low frequency and the integral stainless steel jacket, rather than titanium, provide important new data for this full production model low-beta cavity. The studies include multi-axial magnetic field measurements near the cavity surface due to ambient and applied fields. Cavity performance under different conditions is measured at temperatures ranging between 1.6 K and 4.5 K. A residual resistance of approximately 5-7 nΩ at 1.6 K is observed. Data suggest that an appreciable fraction arises from losses that are not due to flux trapping.

INTRODUCTION

Trapped flux can be a major contributor to the residual resistance of a superconducting cavity. Many studies have been performed on the effects of magnetic field on elliptical superconducting cavity performance examining the effects of ambient field [1, 2], cooling rate through transition [3, 4], thermocurrents [3, 5] and other factors [6].

This paper reports a study of the effects of trapped flux on a low-frequency, TEM-type cavity of a class used in ion accelerators such as those used for the ATLAS heavy-ion accelerator facility at Argonne and FRIB at Michigan State University. Such low frequency TEM cavities differ in geometry and field distribution from elliptical cavities previously studied. Also, the work reported below uses a cavity housed in a stainless-steel (SS) jacket: different from the titanium-niobium system used in most of the earlier reported studies using elliptical-cell cavities. These significant differences motivated this study of static magnetic fields on a low-frequency TEM cavity.

EXPERIMENTAL SETUP

337 MHz HWR Niobium Cavity

A 337 MHz niobium half-wave resonator (HWR) was tested and evaluated under different conditions of magnetic field. The cavity was made with fine grain, RRR=280 niobium manufactured by ATI Specialty Alloys and Components. The parameters of the cavity are shown in Table 1.The entire cavity was encloseded in a stainless steel (SS) helium jacket, as modelled in Fig. 1. The niobium cavity was copper-brazed to the SS outer-jacket at each of the seven coupling and beam ports. Details of the cavity can be found in [7]. There are five coupling ports: two at each end of the cavity, and one at the bottom. Two beam ports are at the center of the cavity with the axes perpendicular to the bottom coupling port as shown in the figure. Two helium inlet ports were placed at the top of the helium jacket, allowing cooling from the cryostat helium reservoir During the cooldown, helium gas was drawn from the top through the relatively small-diameter cooldown port near the bottom of the helium jacket. At each end of the helium jacket, there are two additional access ports. These ports enabled the placement of fluxgate magnetometers within the liquid helium and closely adjacent to the cavity niobium surfaces.

Table 1: Cavity Parameters

Parameter	Value	Unit
Cavity resonant frequency	337	MHz
Effective Length (βλ)	0.26	m
β	0.29	
E_{peak} / E_{acc}	4.5	
B_{peak} / E_{acc}	9.6	mT/(MV/m)
Geometry Factor (R_sQ)	97	
R_{sh}/Q	194	Ω

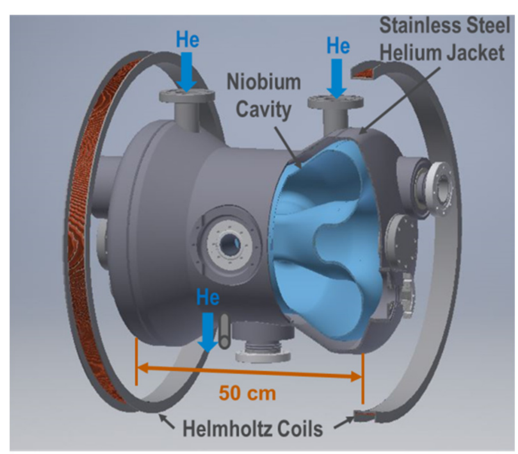

Figure 1: A schematic model of a 337 MHz HWR niobium cavity with Helmholtz coils.

Pior to the tests, the cavity was processed using the standard Argonne recipe, which has been used successfully on many cavities. The cavity was

*This material is based upon work supported by the U.S. Department of Energy, Office of Science, Office of Nuclear Physics, under contract number DE-AC02-06CH11357, and the Office of High Energy Physics, under contract number DE-AC02-76CH03000. This research used resources of ANL's ATLAS facility, which is a DOE Office of Science User Facility.
tng@anl.gov

ISBN: 978-3-95450-211-0 doi:10.18429/JACoW-SRF2019-TUFUB5

electropolished [8], degassed at 625 ºC for 10 hours and high-pressure rinsed.

Temperature and Magnetic Field Measurements

A total of nine silicon diodes were clamped onto the outside surface of the stainless steel flanges on the helium jacket for temperature measurements. Indium was placed between the diodes and the cavity jacket to improve thermal conductivity.

As shown in the dotted rectangles in Fig. 2 (top), five fluxgates were installed inside the helium space through the access ports at the ends of the cavity jacket in order to measure the magnetic fields. Four fluxgates were installed on an insertion platform and inserted through the left helium port. Three of them covered three axes and the other one was set vertically inside a small solenoid coil. The actual set up is shown in Fig. 2 (bottom). A fifth fluxgate was installed near the SS-Nb junction on the other (right) side of the cavity. This fluxgate will be utilized to measure thermocurrent in future investigations.

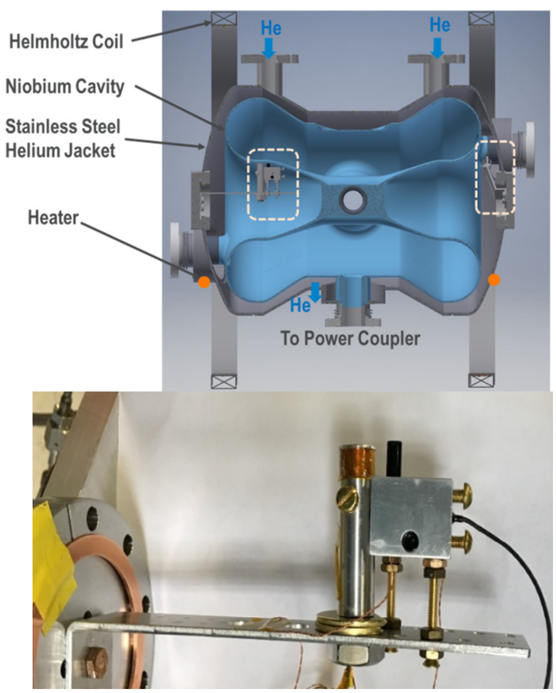

Figure 2: Cross-sectional view of the cavity model and the fluxgate installation, indicated inside the dotted rectangles (top); an actual setup of fluxgate platform (bottom)

Magnetic Field Shielding and Generation

The cryostat in which the cavity was tested provides magnetic shielding, which reduced the ambient magnetic field to 18 ± 1 mG in the region of the cavity. A coil was installed under the cryostat, where a hole on the cryostat magnetic shielding was required to provide access to the cavity for the variable rf power coupler. Adjusting the dc current through the coil provided active shielding and was used in several cases to lower the magnetic field in the region of the cavity to 4 ± 1 mG.

To vary the magnetic field around the cavity, Helmholtz coils were installed with its axis along the cylindrical axis of the cavity, as illustrated in Fig. 1. The generated magnetic field magnitude depends on the current applied and was generally much larger than the ambient field inside the cryostat. In this study, applied fields of 315 mG and 620 mG were generated. Figure 3 shows a CST Microwave Studio simulation of the applied magnitude field distribution over the (normal conducting) cavity. The uniformity of the applied field was estimated to be ±17%.

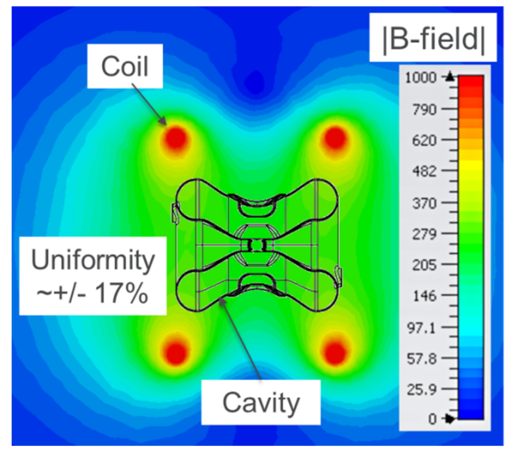

Figure 3: The CST Microwave Studio simulation of the applied magnitude field distribution over the cavity.

Cooling Procedure

To cool the cavity to the testing temperature, i.e. 4.5 K and 1.6 K, the cryostat was pre-cooled by running liquid nitrogen through the heat-shield. Over a period of a couple of days, the cavity cooled by radiation and to about 200K. Then, the cavity was cooled directly by injecting cold helium at the top of the cavity helium vessel and extracting the helium through the cooldown port at the bottom of the cavity helium vessel, as indicated in Fig. 1. Cooling down as rapidly as possible with this scheme, we could cool through the Q-disease region (150–50 K) in about 2 hours. Once below the Q disease region, the temperature was held between 20-30 K by throttling the helium flow. The cavity sat at this temperature for some time to allow rough equilibration of the system before finally cooling through the transition. Cool down through the transition at a designated cooling rate was performed by controlling the flow of LHe. After the transition, the cooling rate of cavity would gradually slow down and stop at 4.5 K with an equilibrium bath pressure of 1040 Torr. For 1.6 K measurement, the refrigerator was disconnected from the test cryostat and the pressure inside the dewar of the cryostat was reduced monotonically by pumping and controlled within a pressure window of 5-6 Torr.

To study magnetic field effects on the cavity required going through the superconducting transition temperature repeatedly with different magnetic fields. Therefore, the cavity needed to be warmed up and cooled down multiple times. To stay below the Q disease zone during the warm-

ISBN: 978-3-95450-211-0 doi:10.18429/JACoW-SRF2019-TUFUB5

up and cool-down, the cavity was warmed up by boiling off LHe and then taken to 20-30K with a pair of 50 W heaters installed at the bottom of the helium jacket, as shown in Fig. 2. After allowing time for temperature of the cavity to stabilize, the cavity was filled with LHe for cool down again. It is believed that this scheme enables the warm up and cool down repeatedly without the deterioration of the cavity performance due to Q disease.

RESULTS AND DISCUSSION

Q Curves

Cavity performance curves (Q vs. E_{ACC}) at 4.5 K and 1.6 K, with and without active field cancellation during cavity transition were measured and are shown in Fig. 4. All Q measurements were obtained with a same electronics and the cavity field gradient was limited to 10 MV/m, the onset of field emission, in order not to introduce unwanted Q degradation. The 1.6 K curves show the observed cavity performance at two fields (17 mG and 5 mG), and also the improvement obtained by the use of active shielding. Initially, the cavity was first cooled through the transition with active cancellation, giving 5 mG ambient field (blue circles). After obtaining the Q curve at 1.6 K, the cavity was warmed above the transition and then cooled down through transition without active shielding, i.e 17 mG ambient field. The 1.6 K Q curve (blue square) shows reduced Q presumably due to additional trapped flux. Both Q curves have similar Q slopes. The offset in the Q curves corresponds to about difference in surface resistance of about 2.4 nΩ.

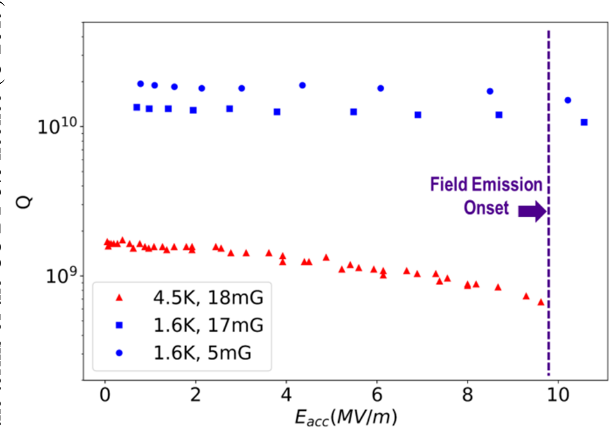

Figure 4: Q curves of the cavity for different temperatures and ambient magnetic fields.

Flux Change Cooling Through T_c

To study the flux expulsion of the Nb cavity during transition, magnetic fields of 315 mG and 620 mG generated with the Helmholtz coils were applied during the cool down through the transition temperature (T_c) as a function of cooling rate. The measured flux changes are shown in Fig. 5. Note that the temperature on the x-axis is measured by a silicon diode attached to the outside of the SS jacket, and not to the niobium cavity surface was would be preferred. For this reason the flux change was observed at a measured temperature slightly higher than the T_c for niobium. This is especially true for the fastest cooldown rate where the niobium cooled before the SS helium jacket. In Figure 4 the x-axis shows the temperature decreasing from left to right, corresponding increasing time. The magnetic field on the y-axis is the magnitude of the field along the applied field direction and was close to the inner-conductor surface of the cavity. Data points were collected at 1-minute intervals. The data points are denser when cooling rate is low and the distance between data points increases with increasing cooling rate. Based on Fig. 5, when the temperature decreases to near T_c, modest flux motion is seen for all cases. There was a factor of more than 10 between the minimum (0.03 K/min) and maximum possible (0.46 K/min) cooling rates in this system. All the measurements indicate about a 2% flux increase. The results show that the flux change of the subject cavity is independent to the cooling rate with this range and of the magnitude of the applied field.

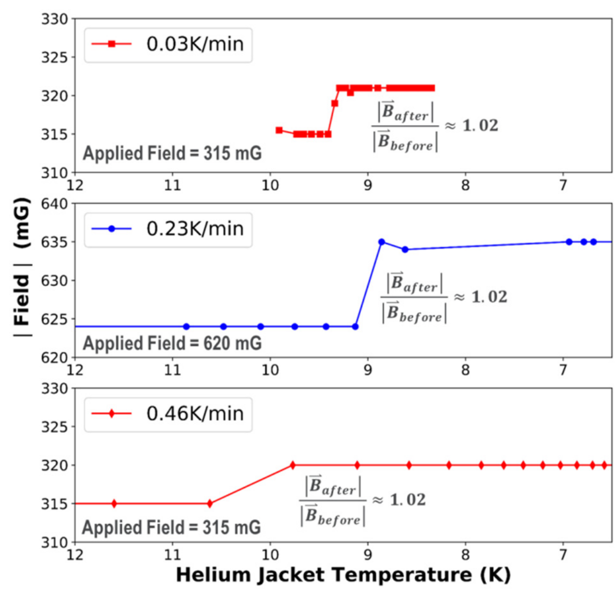

Figure 5: Flux change cooling through Tc with different applied magnetic fields and cooling rates.

Surface Resistance

To look at the dependency of surface resistance on magnetic field from 5 to 620 mG, the surface resistance was calculated with the measured Q at low rf-field and the cavity geometry factor of 97 Ω. Figure 6 shows the surface resistance for different applied magnetic fields ranging from 5 to 620 mG at 4.5 K and from 4 to 18 mG at 1.6 K. The dotted lines show the best-fit linear relationship between the magnitude of the trapped flux and the rf surface resistance. At 4.5 K, we find a sensitivity to trapped flux of 0.19 nΩ/mG. The data points obtained at 1.6 K are shown (magnified) in the bottom graph of Fig. 6. The data at 1.6 K was measured with the applied magnetic field being only the ambient field inside the cryostat both with and without active

ISBN: 978-3-95450-211-0 doi:10.18429/JACoW-SRF2019-TUFUB5

shielding. The surface resistance at 1.6 K is about 5 nΩ for a 5 mG trapped field, and 7 nΩ for 17 mG. This implies a sensitivity at 1.6 K of about 0.17 nΩ/mG. The well-known empirical formula relating the surface resistance due to trapped flux as a function of rf frequency and trapped magnetic field (H_{ext}) [9] is:

$$R_{mag}[n\Omega] = 0.3H_{ext}[mG]\sqrt{f[GHz]}$$

The coefficient of 0.3 in the equation is material dependent and it is for Nb. The extracted coefficient of 0.28 in the present study is, perhaps, surprisingly close.

At 1.6 K, the (BCS) temperature-dependent surface resistance is so small that, within errors, it can be ignored. When we extrapolate the dotted line in Fig. 6 (bottom), this implies a 4.2 nΩ surface resistance at zero field. This is strong evident that the ~4 nΩ of residual resistance is not due to the bulk external magnetic field at 1.6 K. In other words, there is a substantial fraction of residual rf loss is not attributed to the trapped flux, but other, unknown factors.

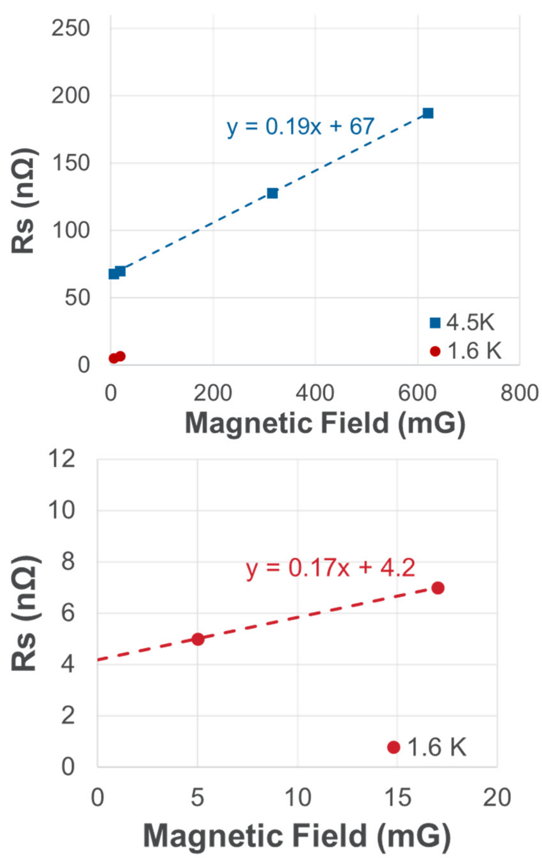

Figure 6: Surface Resistance due to different magnitude field at 4.5 K and 1.6 K (top), magnification of 1.6 K data points (bottom)

SUMMARY

We found very little Meissner effect (flux expulsion) in the subject cavity under the present test conditions. We note, the flux trapping and sensitivity to trapped flux in the subject TEM cavity differs from some TM and TEM cavities reported. We also observe that the flux change on cooling through transition is largely independent of cooling rate between 0.03 and 0.5 K/min cooling rate and also independent of the magnitude of the applied magnetic field.

Further, we observed a ratio of surface resistance to trapped magnetic of 0.17 and 0.19 nΩ/mG at 1.6 K and 4.5 K, respectively: in reasonable agreement with the well-known rule-of thumb; At our lowest achieved 5 mG level, trapped flux may not be the dominant factor affecting the performance of the HWR cavity. Additionally, so far there is no evidence of thermocurrents (< 5 mG induced field) in the subject SS-Nb cavity. We hope to repeat the thermocurrent measurements at a higher resolution.

ACKNOWLEDGEMENTS

The authors would like to acknowledge the considerable efforts for B. Guilfoyle, M. Kedzie, J. Kilbane, T. Reid and G. Zinkann in the assistance on cavity treatment, engineering installation and cavity test.

REFERENCES

[1] C. Vallet *et al.*, “Flux Trapping in Superconducting Cavities”, in *Proc. 3rd European Particle Accelerator Conf. (EPAC'92),* Berlin, Germany, Mar. 1992, pp. 1295-1298.

[2] C. Benvenuti *et al.*, “Magnetic Flux Trapping in Superconducting Niobium”, in *Proc. 8th Int. Conf. RF Superconductivity (SRF'97),* Padova, Italy, Oct. 1997, paper SRF97B05, pp. 331-336.

[3] J. M. Vogt, O. Kugeler, J. Knobloch, “Impact of cool-down conditions at Tc on the superconducting rf cavity quality factor”, *Physical Review Special Topics – Accelerators and Beams*, vol. 16, p. 102002, 2013.

[4] Romanenko, A. Grassellino, O. Melnychuk, D. A. Sergatskov, “Dependence of the residual surface resistance of superconducting radio frequency cavities on the cooling dynamics around Tc”, *Journal of Applied Physics*, vol. 115, p. 184903, 2014.

[5] J. Knobloch, H. Padamsee, “Flux Trapping in Niobium Cavities During Breakdown Events”, in *Proc. 8th Int. Conf. RF Superconductivity (SRF'97),* Padova, Italy, Oct. 1997, paper SRF97B06, pp. 337-344.

[6] M. Martinello *et al.*,“ Magnetic Flux Studies in Horizontally Cooled elliptical Superconducting Cavities”, *Journal of Applied Physics*, vol. 118, p. 044505, 2015.

[7] P. N. Ostroumov *et al.*, “β= 0.285 Half-Wave Resonator for FRIB”, in *Proc. 15th Int. Conf. RF Superconductivity (SRF'11),* Chicago, IL, USA, Jul. 2011, paper MOPO026, pp. 132-134.

[8] T. Reid, S. M. Gerbick, M. P. Kelly, R. C. Murphy, “Current State of Electropolishing at ANL”, in *Proc. 15th Int. Conf. RF Superconductivity (SRF'11),* Chicago, IL, USA, Jul. 2011, paper TUPO021, pp. 408-410.

[9] H. Padamsee, J. Knobloch, T. Hays, “Residual Resistance” in *RF Superconductivity for Accelerators*, Germany: Wiley-VCH, 2009, pp.174.